Directional Initial Access for Millimeter Wave Cellular Systems

C. Nicolas Barati *, S. Amir Hosseini *, Marco Mezzavilla *, Parisa Amiri-Eliasi *
Sundeep Rangan *, Thanasis Korakis *, Shivendra S. Panwar *, Michele Zorzi †
* NYU Tandon School of Engineering, Brooklyn, New York 11201
† University of Padova, Italy
Email:*{nicolas.barati,amirhs.hosseini,pa854,mezzavilla,srangan,korakis,panwar}@nyu.edu, †zorzi@dei.unipd.it

***Abstract*—Communication in millimeter (mmWave) bands seems an evermore promising prospect for new generation cellular systems. However, due to high isotropic pathloss at these frequencies the use of directional antennas becomes mandatory. Directivity complicates many system design issues that are trivial in current cellular implementations. One such issue is initial access, i.e., the establishment of a link-layer connection between a UE and a base station. Based on different combinations of beamforming architectures and transmission modes, we present a series of design options for initial access in mmWave and compare them in terms of delay performance. We show that the use of digital beamforming for initial access will expedite the whole process significantly. Also, we argue that low quantization digital beamforming can more than compensate for high power consumption.**

I. Introduction

The mmWave bands offer orders of magnitude more spectrum than the congested bands in conventional UHF and microwave frequencies below 3 GHz. Hence, they are considered as a suitable candidate for next generation cellular communications. In addition, advances in CMOS RF circuits combined with the small wavelengths of mmWave frequencies enable large numbers of electrically steerable antenna elements to be placed in a picocellular access point or mobile. These high-dimensional antenna arrays can provide further gains via adaptive beamforming (BF) and spatial multiplexing, thus achieving very large capacity [1, 2].

However, much remains to be designed so that cellular systems can exploit the very large capabilities of mmWave bands. This paper considers the basic problem of *initial access* – the procedure by which a mobile (or user equipment (UE) in 3GPP terminology) discovers a potential mmWave cell and establishes a link-layer connection.

mmWave communication relies heavily on highly-directional transmissions to overcome the large isotropic path loss, and this use of directional transmissions significantly complicates initial access. In addition to the mutual detection of the BS and the UE, the mmWave initial access procedure must provide a mechanism by which both the UE and the BS can determine suitable beamforming directions on which subsequent directional communication can be carried out. With very high beamforming gains, this angular search can significantly slow down the initial access. This increase in delay goes against one of the main objectives of mmWave systems, which is to dramatically reduce both data plane and control plane latency [3, 4].

This paper evaluates several different design options for mmWave initial access. We consider the same basic steps as used in the LTE standard, but with different modifications so that both the UE and the BS can learn the initial beamforming directions. The design options consider different methods for transmitting and receiving the synchronization (sync) signals from the BS and the random access (RA) request from the UE. For each option, we evaluate the overall delay for a fixed system overhead of 5%, thereby determining the control plane latency.

We consider the effect of different beamforming architectures available at the BS and the UE. More specifically, we consider both analog and fully digital BF. In the first case the receiver can "look" in only one or a small number of directions at a time, while in the latter it can look in all directions at once. However, digital BF requires as many analog to digital converters (ADC) as the elements of the antenna array. This increases the power consumption to unacceptable levels, especially at the UE side. As a possible solution, we consider low-resolution (say 2-3 bits) ADCs as proposed by [5, 6], showing that they lead to a favorable trade off.

II. Design Options for mmWave Initial Access

A. Initial Access Procedure Steps

All the design options we consider for initial access follow the same basic steps used in 3GPP LTE, which are described in the specifications [7, 8, 9] as well as in any standard text such as [10]. The whole procedure, however, is modified to enable both the UE and the BS to determine the initial beamforming directions in addition to detecting the presence of the BS and access request from the UE. The steps are as follows:

0) *Synchronization signal detection:* Each cell BS periodically transmits synchronization signals that the UE can scan for to detect the presence of the base station and obtain the downlink frame timing. In LTE, the first synchronization signal to detect is the Primary Synchronization Signal (PSS). For mmWave, the synchronization signal will also be used to determine the UE's beamforming direction, which is related to the angles of arrival of the signal paths from the BS. Critical to our analysis, we will assume that the UE only attempts to learn the long-term beamforming

Step	Item	Option	Explanation
0	Sync BS TX	Omni	sync transmitted in a fixed, wide angle beam to cover the entire cell area.
		Directional	sync transmitted in time-varying narrow-beam directions to sequentially scan the angular space.
0	Sync UE RX	Directional	UE listens for the sync signal in time-varying narrow-beam directions with analog BF that sequentially scans the angular space.
		Digital RX	UE has a fully digital RX and can receive in all directions at once.
1	RA BS RX	Directional	The BS listens for the RA signal in time-varying narrow-beam directions with analog BF. that sequentially scans the angular space.
		Digital RX	BS has a fully digital RX and can receive in all directions at once.

TABLE I: Design options for each stage

directions [11], which depend only on the macro-level scattering paths and do not vary with small scale fading. As a result, the long-term beamforming directions will be stable over much longer periods and thus will be assumed to be constant over the duration of the initial access procedure.

1) *RA preamble transmission:* Similar to LTE, we assume that the uplink contains dedicated slots exclusively for the purpose of random access messages. After detecting the synchronization signal and decoding the broadcast messages, the locations of these RA slots are known to the UE. The UE randomly selects one of a small number (in LTE, there are up to 64) waveforms called *RA preambles* and transmits the preamble in one of the RA slots. In all design options we consider below, the UE BF direction is known after step 0, so the RA preamble can be transmitted directionally, thereby obtaining the BF gain on the UE side. The BS will scan for the presence of the RA preamble and will also learn the BF direction on the BS side. As we discuss below, the method by which the BS will learn the BF direction will depend on the RA procedure.
2) *Random access response (RAR):* Upon detecting a RA preamble, the base station transmits a random access response to the UE indicating the index of the detected preamble. At this point, both the BS and the UE know the BF directions so all transmissions can obtain the full BF gain.
3) *Connection request:* After receiving RAR, the UE desiring initial access will send some sort of connection request message on the resources scheduled in the uplink (UL) grant in the RAR. In 3GPP LTE, this message is contained in the "Radio Resource Control (RRC) connection request" and contains, among other data, authentication and identification information for the UE.
4) *Connection setup and contention resolution:* At this point, all subsequent communications can occur on scheduled channels with the full BF gain on both sides. In 3GPP LTE, the immediate subsequent messages would be used for connection set up and contention resolution.

B. Design Options for Learning the BF Directions

The key modifications to enable learning the initial communication directions would occur in steps 0 and 1 of the initial access as described above. In step 0, the UE must learn its BF direction, and in step 1 the BS learns the BF direction on its side. The remaining steps are likely to be largely similar to the LTE procedure and thus are not considered in detail here. Table I shows some options for three items in this procedure, namely: (i) the manner in which the synchronization signal in step 0 is transmitted by the BS; (ii) the manner in which the synchronization signal is received at the UE; and (iii) the manner in which the random access preamble from the UE is received at the BS in step 1. For each item, we consider two possible options. For example, for the manner in which the synchronization signal is transmitted, we consider a fixed omni-directional transmission or a sequential scanning with directional transmissions.

Now, since there are two options for each of the three items in Table I, there are a total of eight design option combinations. However, we consider only five of these options since the three options left out were found to have similar performance as at least one of the five presented.

The option combinations we consider are as follows [1]. They are named after the manner of the sync signal transmission and reception in step 0 of the initial access procedure, and RA preamble reception in step 1. For example *DDO* refers to the scheme where the sync signal is transmitted and received directionally but the RA preamble is received omnidirectionally.

a) *DDO:* Here, step 0, i.e. sync signal transmission and reception is done directionally in the analog domain. Step 1, on the other hand, that is RA reception, is done omnidirectionally. The index of the time slot in which the UE received the sync signal is encoded in the RA preamble index. This way, the BS learns the TX direction in which the sync signal was received.
b) *DDD:* Step 0 is performed as in *DDO* but step 1 is done directionally in the analog domain. Since the BS scans the directions for the RA preamble, the BF direction can be learned from the direction in which the RA preamble is received.
c) *ODD:* In step 0 the sync signal is transmitted omnidirectionally but received directionally. Step 1 is identical to *DDD*.
d) *ODDig:* Step 0 is similar to *ODD* but in step 1 the BS receives the RA preamble using digital BF. Using digital BF enables the BS to have access to all the spatial samples at once, and hence learn the incoming direction in one measurement time.

[1]Note that the option combinations considered include designs proposed in the recent works [12] and [13]

e) *ODigDig:* In step 0, the sync signal is transmitted omnidirectionally but is received at the UE with digital BF. Hence, the UE can learn the incoming direction at once. Step 1 is identical to *ODDig*.

For the digital cases we will assume low quantization ADCs (2-3 bits) to compensate for using many of these power consuming elements.

III. Signal Detection under a Sequential Beamspace Scanning

A. Sequential Beamspace Scanning

We can analyze both the synchronization and the RA phase with the same analysis. Suppose a transmitter (TX: BS in step 0 or UE in step 1) repeatedly broadcasts some known signal once every $T_{\rm per}$ seconds. For frequency diversity, we assume that each transmission consists of $N_{\rm div}$ *sub-signals* transmitted in different frequency locations and that these sub-signals and their frequency locations are known to the receiver. The sub-signals are assumed to be mostly constrained to some small time-frequency region of size $T_{\rm sig} \times W_{\rm sig}$, where $T_{\rm sig}$ and $W_{\rm sig}$ are the sub-signal duration and bandwidth. The goal of the receiver is to detect the presence of the signal, and, if it is present, detect its time and angle of arrival.

Now, for the moment, suppose that both the TX and the RX can perform only analog BF, so that they can only align their arrays in one direction at a time (including omnidirectional operation). To detect the synchronization signal, we assume that the TX and the RX cycle through L possible TX-RX BF direction pairs. We will call each such cycle of L transmissions a "directional scan" or " scan cycle." Since the transmission period is $T_{\rm per}$ seconds, each scan cycle will take $LT_{\rm per}$ seconds. We index the transmissions in each scan cycle by $\ell = 1, \ldots, L$, and let $\mathbf{u}_\ell$ and $\mathbf{v}_\ell$ be the RX and TX beamforming vectors applied in the ℓ-th transmission in each scan cycle. The same beamforming vectors are applied to all sub-signals in each transmission.

In this work, we will assume a simple *beamspace* sequential search. Given a linear or 2D planar array with N antennas, the spatial signature of any plane wave on that array is given by a superposition of N orthogonal directions called the beamspace directions. Each beamspace direction corresponds to a direction of arrival at a particular angle. In beamspace scanning, the TX and RX directions that need to be searched are selected from the orthogonal beamspace directions. If the TX and RX have $N_{\rm tx}$ and $N_{\rm rx}$ antennas, respectively, then the number L of directions to scan is given by:

- $L = N_{\rm tx}N_{\rm rx}$ if both the TX and RX scan over all the beamspace directions;
- $L = N_{\rm tx}$ if only the TX scans while the RX uses an omni-directional or fixed antenna pattern;
- $L = N_{\rm rx}$ if only the RX scans while the TX uses an omni-directional or fixed antenna pattern;
- $L = 1$ if both the TX and RX use omni-directional or fixed antenna patterns.

The TX and RX continue repeating the transmission scans until either the signal is detected or the procedure times out.

B. Generalized likelihood ratio test Detection

Given the above transmissions, the RX must determine whether the signal is present, and, if so, its the direction of maximum energy. To make this decision, suppose that the RX listens to K scan cycles for a total of LK transmissions. Index the transmissions within each scan cycle by $\ell = 1, \ldots, L$ and the cycles themselves by $k = 1, \ldots, K$. We let $\mathbf{s}_{\ell d} \in \mathbb{C}^M$ be the signal space representation with M degrees of freedom of the d-th sub-signal transmitted in the ℓ-th transmission in each scan cycle where $d = 1, \ldots, N_{div}$. If the sub-signal can be localized to a time interval of length $T_{\rm sig}$ and bandwidth $W_{\rm sig}$, then $M \approx T_{\rm sig}W_{\rm sig}$.

We assume that in the ℓ-th transmission within each scan cycle, the RX and TX apply the beamforming vectors $\mathbf{u}_\ell \in \mathbb{C}^{N_{\rm rx}}$ and $\mathbf{v}_\ell \in \mathbb{C}^{N_{\rm tx}}$. We also assume that the received complex baseband signal in the d-th sub-signal in the ℓ-th transmission and k-th scan cycle is modeled as

$$\mathbf{r}_{k\ell d} = \mathbf{u}_\ell^* \mathbf{H}_{k\ell d}\mathbf{v}_\ell \mathbf{s}_{\ell d} + \mathbf{w}_{k\ell d}, \quad \mathbf{w}_{k\ell d} \sim \mathcal{N}(0, \tau_{k\ell d}\mathbf{I}_M), \quad (1)$$

where $\mathbf{r}_{k\ell d} \in \mathbb{C}^M$ is the signal space representation of the received sub-signal after beamforming; $\mathbf{H}_{k\ell d}$ is the complex MIMO fading channel matrix during the transmission, and $\mathbf{w}_{k\ell d}$ is complex white Gaussian noise (WGN) with some variance $\tau_{k\ell d}$ in each dimension. We consider the channel flat during each sub-signal transmission.

Our first key simplifying assumption is that the true channel between the TX and RX, if it exists, is described by a single line-of-sight (LOS) path exactly aligned with one of the L TX-RX beamspace directions. That is,

$$\mathbf{H}_{k\ell d} = h_{k\ell d}\mathbf{u}_{\ell_0}\mathbf{v}_{\ell_0}^*, \quad (2)$$

so that the channel's TX direction $\mathbf{v}_{\ell_0}$ and RX direction $\mathbf{u}_{\ell_0}$ are each aligned exactly on one of the TX and RX beamspace directions, $\mathbf{v}_\ell$ and $\mathbf{u}_\ell$. $h_{k\ell d}$ is a scalar small-scale frequency selective (along the much larger data bandwidth) fading coefficient that may vary with the sub-signal d, transmission ℓ and scan cycle k. This simplifying assumption is used only in deriving the detectors and is relaxed in our performance analysis and simulations where we use a realistic measurement-based channel model.

Now, if we assume that the beamforming directions are orthonormal, i.e., $\mathbf{u}_\ell^*\mathbf{u}_{\ell_0}\mathbf{v}_\ell^*\mathbf{v}_{\ell_0} = \delta_{\ell,\ell_0}$, We can rewrite (1) as

$$\mathbf{r}_{k\ell d} = \psi_{kd}\delta_{\ell,\ell_0}\mathbf{s}_{\ell d} + \mathbf{w}_{k\ell d}, \quad (3)$$

where $\psi_{kd} = h_{k\ell_0 d}$. The variable ψ_{kd} is the complex gain on the d-th sub-signal in the k-th scan cycle at the time when the beam directions are properly aligned.

The detection problem can then be posed as a hypothesis testing problem. Specifically, the presence or absence of the signal corresponds to two hypotheses:

$$\begin{array}{ll} H_0: & \psi_{kd} = 0 \quad \text{(signal absent)}, \\ H_1: & \psi_{kd} \neq 0 \quad \text{(signal present)}. \end{array} \quad (4)$$

Now, the model (3) specifies the probability distribution of the observed data, which we denote as

$$p(\mathbf{r}|\boldsymbol{\tau}, \boldsymbol{\psi}, \ell_0), \quad (5)$$

where $\mathbf{r} = \{\mathbf{r}_{k\ell d}\}$ is the set of all measurements, $\boldsymbol{\tau} = \{\tau_{k\ell d}\}$ is the set of noise levels, $\boldsymbol{\psi} = \{\psi_{kd}\}$ is the set of signal levels and ℓ_0 is the true direction. Since the model has unknown parameters, we follow the procedure in [14] and use a standard Generalized Likelihood Ratio Test (GLRT) [15] to decide between the two hypotheses.

We use the test

$$\widehat{H} = \begin{cases} 1 & \Lambda_0 - \Lambda_1 \geq t \\ 0 & \Lambda_0 - \Lambda_1 < t, \end{cases} \tag{6}$$

where Λ_0 and Λ_1 are the minimum negative likelihoods of each hypothesis, and t is a threshold. It is shown in [16] that the test can be computed as follows. For each transmission ℓ in scan cycle k, we compute the correlation $\rho_{k\ell d}$ which represents the fraction of the received energy due to the transmitted signal. This is simply a matched filter. We next compute the optimal beamspace direction by minimizing

$$\widehat{\ell_0} = \underset{\ell=1,\ldots,L}{\arg\min} \sum_{k=1}^{K} \sum_{d=1}^{N_{div}} \ln\left(1 - \rho_{k\ell d}\right). \tag{7}$$

Then, the log likelihood difference is given by [16]

$$\Lambda_0 - \Lambda_1 = M \sum_{k=1}^{K} \sum_{d=1}^{N_{div}} \ln\left(1 - \rho_{k\widehat{\ell_0} d}\right), \tag{8}$$

which can be applied into the hypothesis test (6).

C. Digital Beamforming

The above detector was derived for the case of analog BF. However, the same detector can be used for digital BF [16]. For digital BF, one can simply test all N_{rx} directions in each time step, which is again equivalent to analog BF but with an even faster acceleration. Of course, as discussed earlier, digital BF may require higher power consumption to support separate ADCs for each antenna element. Since the power consumption of an ADC generally scales as 2^b, where b is the number of bits [17], we will constrain the fully digital architecture to have at most $b = 3$ bits per I/Q dimension. Since conventional ADCs typically have close to 10 bits, using 3 bits will reduce the power consumption by a factor of 128; which more than compensates for adding an ADC to all the 16 or 64 elements of the antenna array with minimal SNR loss in the critical low SNR regime.

IV. Evaluation and Analysis

Given the search algorithm, we can now evaluate each of the design options presented in Section II-B through simulation. The main objective of the simulations is the assessment of each of the options in terms of two delay parameters: (1) The *synchronization delay*, i.e., the time it takes the UE to detect the presence of the synchronization signal in step 0, and (2) the *preamble detection delay*, i.e., the time the BS needs to reliably detect the random access preamble in step 1.

We simulate the detectors' performance for a multipath pathloss channel model [1] derived from actual measurements at 28 GHz in New York City [18, 19, 20]. The detection performance depends on the SNR. Here we focus on the initial access for the crucial case of a typical edge user. That is the user who is in an SNR regime where the mmWave BS can provide a minimum target data rate, after the link-layer connection is established (this is also the case analyzed in [14]).

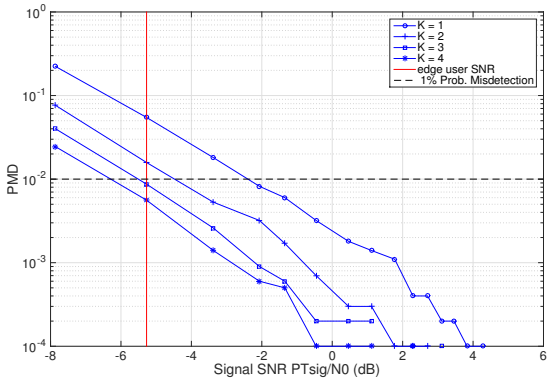

Fig. 1: DDD/DDO, probability of misdetection (P_{MD}) versus synchronization signal SNR for K = 1; 2; 3; 4. Each additional cycle decreases the misdetection probability for a given SNR regime.

The basic parameters of our Monte Carlo simulations are as follows. The BS transmits at a power of 30 dBm in downlink and the UE at 20 dBm in uplink. Both the BS and the typical edge user are equipped with uniform planar antenna arrays (UPA) of size 64 and 16, respectively. For each design option, these array sizes will define the number of directions L in each cycle k that both parties need to scan (see Section III-A). For example, in the case of sync in DDD/DDO, L will be equal to $N_{\text{tx}}N_{\text{rx}} = 1024$. The sync signal and the RA preambles are transmitted with a periodicity $T_{per} = 200$ μs in $N_{\text{div}} = 4$ frequency block of size $W_{\text{sig}} = 1$ MHz of the total 1 GHz system bandwidth. The duration of each sub-signal T_{sig} is chosen to be equal to 10 μs, which is much smaller than the coherence time of the channel in the high mmWave frequencies [18, 19] even for scenarios where the UE is moving with relatively high speed. This duration means that the overhead of each signal transmission (assuming no other signal is transmitted during sync and RA) is 5%. Details of computing the threshold used in comparing the two hypotheses are omitted here due to space limitations. We refer the reader to [16] for a detailed discussion on the appropriate threshold and other parameters and assumptions of our simulations.

A. Synchronization Delay

We now proceed to evaluate the delays for each of the proposed options. We estimate the number of scan cycles K it takes to reliably detect the synchronization signal from the BS. This depends on the design option and the SNR. As an example we show in Figure 1 the probability of misdetection (P_{MD}) as a function of the SNR and the number of scan cycles K for the DDD/DDO design options based on Monte Carlo simulations. Note that the x axis is the sub-signal SNR and not the SNR over the whole available bandwidth which we assume to be much larger than W_{sig}. The false alarm rate was set to $R_{FA} = 0.01$ per scan cycle. We also plotted the vertical

Option	T_{sig}	L		1% SNR			
		Sync	RA	Sync		RA	
				$K*$	delay	$K*$	delay
DDO	10 μs	1024	1	3	614.4	2393	478.6
DDD	10 μs	1024	64	3	614.4	24	307.2
ODD	10 μs	16	64	73	233.6	24	307.2
ODDig	10 μs	16	1	73	233.6	25	5
ODigDig	10 μs	1	1	79	15.8	25	5

TABLE II: Detection delays in milliseconds for a fixed overhead of 5%. The third and fourth column show the minimum required measurements L, when $K = 1$. K^* is the number of full cycles required for detection in each scenario. Values for digital BF are derived given an ADC with 3 bit resolution.

line for the SNR at which the user will receive the sync signal. We set a target mis-detection rate of $P_{MD} = 0.01$ for a sync signal of duration $T_{\text{sig,sync}} = 10$ μs. As we show in the figure, edge users require $K = 3$ scan cycles to meet the target.

We evaluated the sync delay for the rest of the schemes in the same way. The results are summarized in Table II (sync columns). One can see that in general it is better to send the sync signal omnidirectionally. This is evident when comparing for example ODD to DDD/DDO. This gap is due to the large beam space L when both sides are scanning in narrow beams. Another observation is that low-bit resolution digital reception at the UE outperforms the other options by a very large margin.

B. Random Access Delay

For the Random access phase, we perform a detection procedure similar to that for synchronization. We consider the same edge user SNR regime as before. Table II summarizes the results of our RA simulations (RA column). Note that in the RA phase, the UE already knows where the BS is in the angular domain. This means that the number of directions L is always smaller than in the sync phase. While L in sync may range between one and 1024, in RA L will be either 64 or one, depending on the design option.

As in synchronization, digital RX is always a better choice. It brings orders of magnitude better performance in terms of delay in step 1 (5 ms versus more than 300 ms). In addition, using 3-bit ADCs more than compensates for the increased power demand and complexity of digital BF, thereby avoiding the energy consumption drawback often mentioned for this solution and making it a viable option.

V. Findings and Conclusions

While directional transmissions are essential for mmWave, they may significantly delay initial access, especially in the cases where analog directional scanning is used. In general, it is better to send the sync signal in step 0 omnidirectionally regardless of the BF architecture used at the UE. Digital BF is shown to have a great value in initial access, and broadly speaking in the control plane. We can obtain access delays of a few milliseconds – an order of magnitude faster than the control plane latency of approximately 80 ms experienced in LTE. This possibility suggests that mmWave systems enabled with low-resolution fully digital transceivers can not only offer dramatically improved data rates and lower data plane latency but significantly reduce control plane latency as well. Future work can study how systems can be best designed to exploit this capability, particularly for inter-RAT handover, aggressive use of idle modes and fast recovery from link failure.

References

[1] M. Akdeniz, Y. Liu, M. Samimi, S. Sun, S. Rangan, T. Rappaport, and E. Erkip, "Millimeter wave channel modeling and cellular capacity evaluation," , *IEEE Journal on Selected Areas in Communications*, vol. 32, no. 6, pp. 1164–1179, June 2014.

[2] T. Bai and R. Heath, "Coverage and rate analysis for millimeter-wave cellular networks," *IEEE Trans. Wireless Communications*, vol. 14, no. 2, pp. 1100–1114, Feb 2015.

[3] F. Boccardi, R. Heath, A. Lozano, T. Marzetta, and P. Popovski, "Five disruptive technology directions for 5G," *IEEE Communications Magazine*, vol. 52, no. 2, pp. 74–80, February 2014.

[4] T. Levanen, J. Pirskanen, and M. Valkama, "Radio interface design for ultra-low latency millimeter-wave communications in 5G era," in *Proc. IEEE Globecom Workshops*, 2014, pp. 1420–1426.

[5] H. Zhang, S. Venkateswaran, and U. Madhow, "Analog multitone with interference suppression: Relieving the ADC bottleneck for wideband 60 GHz systems," in *Proc. IEEE Globecom*, Nov. 2012.

[6] D. Ramasamy, S. Venkateswaran, and U. Madhow, "Compressive tracking with 1000-element arrays: A framework for multi-Gbps mm wave cellular downlinks," in *50th Annual Allerton Conference on Communication, Control, and Computing (Allerton)*, Oct 2012, pp. 690–697.

[7] 3GPP, "Evolved Universal Terrestrial Radio Access (E-UTRA) and Evolved Universal Terrestrial Radio Access Network (E-UTRAN); Overall description; Stage 2," TS 36.300 (release 10), 2010.

[8] ——, "Evolved Universal Terrestrial Radio Access (E-UTRA) and Evolved Universal Terrestrial Radio Access Network (E-UTRAN); Medium Access Control (MAC) protocol specification," TS 36.321, 2015.

[9] ——, "Evolved Universal Terrestrial Radio Access (E-UTRA) and Evolved Universal Terrestrial Radio Access Network (E-UTRAN); Radio Resource Control (RRC) protocol specification," TS 36.331, 2015.

[10] E. Dahlman, S. Parkvall, J. Sköld, and P. Beming, *3G Evolution: HSPA and LTE for Mobile Broadband*. Oxford, UK: Academic Press, 2007.

[11] A. Lozano, "Long-term transmit beamforming for wireless multicasting," in *Proc. ICASSP*, vol. 3, 2007, pp. III–417–III–420.

[12] C. Jeong, J. Park, and H. Yu, "Random access in millimeter-wave beamforming cellular networks: issues and approaches," *IEEE Communications Magazine*, vol. 53, no. 1, pp. 180–185, Jan 2015.

[13] H. Shokri-Ghadikolaei, C. Fischione, G. Fodor, P. Popovski, and M. Zorzi, "Millimeter wave cellular networks: A MAC layer perspective," *IEEE Transactions on Communications*, vol. 63, no. 10, pp. 3437–3458, Oct 2015.

[14] C. Barati Nt., S. Hosseini, S. Rangan, P. Liu, T. Korakis, S. Panwar, and T. Rappaport, "Directional cell discovery in millimeter wave cellular networks," *to appear in IEEE Transactions on Wireless Communication*.

[15] H. L. Van Trees, *Detection, Estimation and Modulation Theory, Part I*. New York, NY: Wiley, 2001.

[16] C. N. Barati, S. A. Hosseini, M. Mezzavilla, S. Rangan, T. Korakis, S. S. Panwar, and M. Zorzi, "Directional initial access for millimeter wave cellular systems," *arXiv preprint arXiv:1511.06483*, 2015.

[17] B. Razavi, *Design of Analog CMOS Integrated Circuits*. McGraw Hill, 2003.

[18] Y. Azar, G. Wong, K. Wang, R. Mayzus, J. Schulz, H. Zhao, F. Gutierrez, D. Hwang, and T. Rappaport, "28 GHz propagation measurements for outdoor cellular communications using steerable beam antennas in New York City," in *IEEE International Conference on Communications (ICC)*, June 2013, pp. 5143–5147.

[19] H. Zhao, R. Mayzus, S. Sun, M. Samimi, J. Schulz, Y. Azar, K. Wang, G. Wong, F. Gutierrez, and T. Rappaport, "28 Ghz millimeter wave cellular communication measurements for reflection and penetration loss in and around buildings in New York City," in *IEEE International Conference on Communications (ICC)*, June 2013, pp. 5163–5167.

[20] M. Samimi, K. Wang, Y. Azar, G. N. Wong, R. Mayzus, H. Zhao, J. K. Schulz, S. Sun, F. Gutierrez, and T. S. Rappaport, "28 GHz angle of arrival and angle of departure analysis for outdoor cellular communications using steerable beam antennas in New York City," in *Proc. IEEE VTC*, 2013.